5527

Rigid Motion Correction in MRSI Using Wireless Active Markers

Yibo Zhao[1], Chao Ma[2], Chang Gao[1], Kui Ying[1], Jinsong Ouyang[2], and Georges El Fakhri[2]

[1]Engineering Physics, Tsinghua University, Beijing, People's Republic of China, [2]Gordon Center for Medical Imaging, Radiology, Massachusetts General Hospital, Harvard Medical School, Boston, MA, United States

Synopsis

For brain imaging, even with head restraints, maximum translations in the range of 5-10 mm and rotations of 1-4 degrees are sometimes observed. The rigid body motion of the subject during MRSI acquisition can degrade both the spatial resolution and spectral quality. In this work, we developed a wireless active marker based method to track and correct motion in MRSI.

Purpose

For brain imaging, even with head restraints, maximum translations in the range of 5-10 mm and rotations of 1-4 degrees are sometimes observed. This is particularly true in the elderly, with increased significance in patients with dementia or movement disorders. The rigid body motion of the subject during MRSI acquisition can degrade both the spatial resolution and spectral quality. It is increasingly important to correct motion in MRSI with the recent rapid development in high-resolution MRSI techniques[1-6]. Many methods have been proposed to address this issue, e.g., optical motion tracking systems[7-9] and MR navigators[10-13]. However, the optical tracking system requires dedicated hardware, while the MR navigators limit the minimum possible TR, which becomes critical when FID based MRSI sequence is used for fast acquisition. In this work, we developed a wireless active marker based method[14-16] to track and correct motion in MRSI.

Methods

Each of the three MR wireless active markers was made of a spherical micro-sample enclosed by a solenoidal micro-coil (Fig. 1a). The micro-coils were tuned to the resonance frequency of water at 3T. The signals in the micro-sample cell were excited and received through the inductive coupling between the micro-coils and the scanner's transmit and receive coils. A customized echo-planar spectroscopic imaging (EPSI) sequence was modified to acquire projection signals along three orthogonal directions with small flip-angle excitation (<1°) at the end of each TR (Fig. 1b). Besides readout gradients, dephaser gradients were applied to suppress signal outside the active markers. The total acquisition time of the navigator signals was ~15 ms. Fig. 1c shows the navigator signals acquired in a TR. The locations of the markers, which correspond to the individual peaks, are clearly identifiable.

Denoting the positions of the active markers before and after a given movement as $\mathbf{x}$ and $\mathbf{x}'$, respectively, we estimated rigid motion parameters using: $\arg\min_{\mathbf{R},\mathbf{T}} \parallel \mathbf{R}\mathbf{x} + \mathbf{T} - \mathbf{x}' \parallel_2^2$, where $\mathbf{R}$ and $\mathbf{T}$ denote the rotation and translation matrix, respectively. With the estimated rigid motion information, we performed retrospective motion correction in MRSI reconstruction using: $\arg\min_{\boldsymbol{\rho}(\mathbf{x},t)} \sum_n \parallel \Omega_n \mathcal{F}\{\mathcal{T}_n\{\mathcal{R}_n\{\boldsymbol{\rho}(\mathbf{x},t)\}\}e^{-i\omega_n(\mathbf{x})t} - \mathbf{d}_n \parallel_2^2$, where the k-space data were grouped into different segments based on the measured motion information: For the nth segment, $\mathbf{d}_n$, $\mathcal{R}_n$, $\mathcal{T}_n$, $\omega_n(\mathbf{x})$, and Ω_n are the measured motion displacement, estimated rotation, estimated translation, field inhomogeneity, and k-space sampling pattern, respectively.

Results

We carried out a water phantom study with three imaging sessions on a 3T Siemens Trio scanner (Siemens Medical Systems, Erlangen, Germany) to validate the proposed method. For each session, fully sampled high-resolution MRSI data (72x72x24 spatial encodings, single average) were acquired using a customized FID-EPSI sequence (TR/TE=350/4.6ms). B0 inhomogeneity maps were also acquired. Between the sessions, the phantom was translated and rotated manually. To test motion correction, a fully sampled but motion-corrupted MRSI data set was simulated by retrospectively extracting k-space data from each of the three imaging sessions.

Figures 2 and 3 show motion correction results obtained using the high-resolution MRSI data sets. The proposed method significantly reduced the motion artifacts in the spatial domain and the spectral distortion in the spectral domain.

Discussions and Conclusions

A wireless active marker based method has been developed for motion correction in MRSI. Our phantom study shows that the proposed method can accurately track the rigid motion of the imaging object. One remaining issue is to correct B0 inhomogeneity. This can be achieved by dynamically updating the shimming parameters or by acquiring new B0 inhomogeneity maps whenever a large motion detected.

Acknowledgements

This work was support in part by: Tsinghua Top Open Program for Undergraduate Performing Research Abroad and by the National Institutes of Health; Grant: R21EB021710

References

1. Lam F, Liang ZP. A subspace approach to high-resolution spectroscopic imaging. Magn Reson Med 2014;71:1349–1357.

2. Lam F, Ma C, Clifford B, Johnson CL, Liang ZP. High-Resolution 1H- MRSI of the Brain Using SPICE: data Acquisition and Image Reconstruction. Magn Reson Med 2016;76:1059-1070.

3. Ma C, Lam F, Ning Q, Johnson CL, Liang ZP. High-resolution 1H-MRSI of the brain using short-TE SPICE. Magn Reson Med 2016, doi: 10.1002/mrm.26130.

4. Zhang Y, Gabr RE, Schar M, Weiss RG, Bottomley PA. Magnetic resonance spectroscopy with linear algebraic modeling (SLAM) for higher speed and sensitivity. J Magn Reson 2012;218:66–76.

5. Chatnuntawech I, Bilgic B, Adalsteinsson E. Undersampled spectroscopic imaging with model-based reconstruction. In Proceedings of the International Symposium on Magnetic Resonance in Medicine, Salt Lake City, Utah, USA, 2013. p. 3960.

6. Kasten J, Lazeyras F, Van De Ville D. Data-driven MRSI spectral localization via low-rank component analysis. IEEE Trans Med Imaging 2013;32:1853–1863.

7. Andrews-Shigaki BC, Armstrong BS, Zaitsev M, Ernst T. Prospective motion correction for magnetic resonance spectroscopy using single camera Retro-Gratereflector optical tracking. J. Magn Reson Imaging 2011;33:498–504.

8. Lange T, Maclaren J, Buechert M, Zaitsev M. Spectroscopic imaging with pro- spective motion correction and retrospective phase correction. Magn Reson Med 2012;67:1506–1514.

9. Zaitsev M, Speck O, Hennig J, Buchert M. Single-voxel MRS with prospective motion correction and retrospective frequency correction. NMR Biomed 2010;23:325–332.

10. Hess AT, Tisdall MD, Andronesi OC, Meintjes EM, van der Kouwe AJW. Real-time motion and B0 corrected single voxel spectroscopy using volumetric navigators. Magn Reson Med 2011;66, 314–323.

11. Hess AT, Andronesi OC, Tisdall MD, Sorensen AG, van der Kouwe AJW, Meintjes EM. Real-time motion and B-0 correction for localized adiabatic selective refocusing (LASER) MRSI using echo planar imaging volumetric navigators. NMR Biomed 2012; 25: 347–358.

12. Thiel T, Czisch M, Elbel GK, Hennig J. Phase coherent averaging in magnetic res- onance spectroscopy using interleaved navigator scans: compensation of motion artifacts and magnetic field instabilities. Magn Reson Med 2002; 47: 1077–1082.

13. Bogner W, Hess AT, Gagoski B, Tisdall MD, van der Kouwe AJW, Trattnig S, Rosen B, Andronesi OC. Real-time motion- and B0-correction for LASER-localized spiral-accelerated 3D-MRSI of the brain at 3 T. NeuroImage 2014;88:22-31.

14. Ackerman J, Offutt M, Buxton R, Brady T, Rapid 3D tracking of small RF coils. In Proc Soc Magn Reson Med 1986, pp. 1131–1132.

15. Huang C, Ackerman JL, Petibon Y, Brady TJ, El Fakhri G, Ouyang J, MR-based motion correction for PET imaging using wired active MR microcoils in simultaneous PET-MR: Phantom study. Med Phys 2014;41:041910.

16. Huang C, Ackerman JL, Petibon Y, Normandin M, Brady TJ, El Fakhri G, Ouyang J, Motion compensation for brain PET imaging using wireless MR active markers in simultaneous PET–MR: Phantom and non-human primate studies. Neuroimage 2014;91:129-137.

Figures

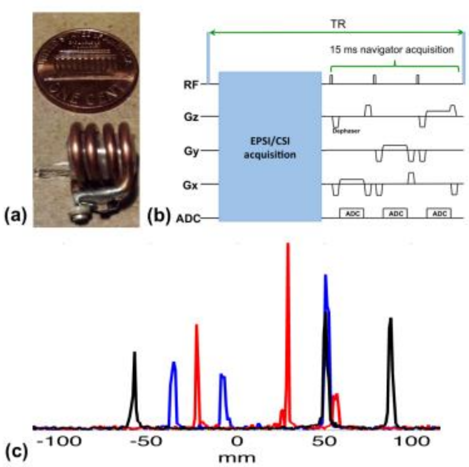

Figure 1. (a) Wireless microcoils for motion tracking. (b) MRSI acquisition with navigators to obtain motion information from the microcoil. (c) Measured navigator signals along three projection axes.

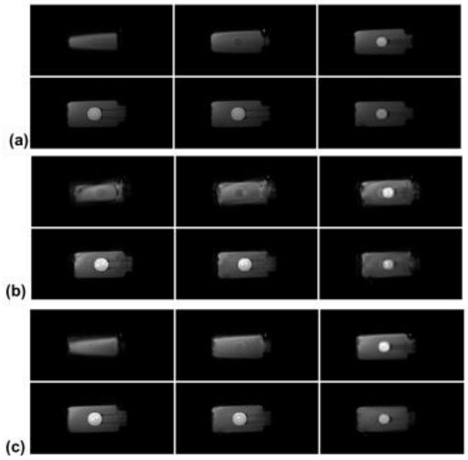

Figure 2. The first-echo images of (a): Fourier reconstruction of a motion-free MRSI data, (b) Fourier reconstruction of a motion-corrected MRSI data, and (c) Motion corrected reconstruction of the data in (b).

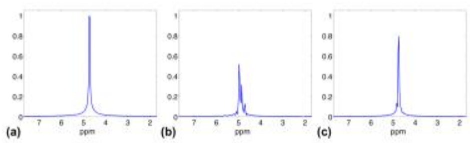

Figure 3. Representative spectra of water, corresponding to Figs. 2a to 2c.